

Incipient melt formation and devitrification at the Wanapitei impact structure, Ontario, Canada

B. O. DRESSLER^{1*}, D. CRABTREE² AND B. C. SCHURAYTZ^{1,3}

¹Lunar and Planetary Institute, 3600 Bay Area Boulevard, Houston, Texas 77058-1113, USA

²Geoscience Laboratories, Ontario Geoservices Centre, 933 Ramsey Lake Road, Sudbury, Ontario P3E 6B5, Canada

³Present address: Planetary Science Branch, SN4, NASA Johnson Space Center, Houston, Texas 77058, USA

*Correspondence author's e-mail address: dressler@lpi.jsc.nasa.gov

(Received 1995 October 5; accepted in revised form 1996 December 5)

Abstract—The Wanapitei impact structure is ~8 km in diameter and lies within Wanapitei Lake, ~34 km northeast of the city of Sudbury. Rocks related to the 37 Ma impact event are found only in Pleistocene glacial deposits south of the lake. Most of the target rocks are metasedimentary rocks of the Proterozoic Huronian Supergroup. An almost completely vitrified, inclusion-bearing sample investigated here represents either an impact melt or a strongly shock metamorphosed, pebbly wacke. In the second, preferred interpretation, a number of partially melted and devitrified clasts are enclosed in an equally highly shock metamorphosed arkosic wacke matrix (*i.e.*, the sample is a shocked pebbly wacke), which records the onset of shock melting. This interpretation is based on the glass composition, mineral relicts in the glass, relict rock textures, and the similar degree of shock metamorphism and incipient melting of all sample components. Boulder matrix and clasts are largely vitrified and preserve various degrees of fluidization, vesiculation, and devitrification. Peak shock pressure of ~50–60 GPa and stress experienced by the sample were somewhat below those required for complete melting and development of a homogeneous melt. The rapid cooling and devitrification history of the analyzed sample is comparable to that reported recently from glasses in the suevite of the Ries impact structure in Germany and may indicate that the analyzed sample experienced an annealing temperature after deposition of somewhere between 650 °C and 800 °C.

INTRODUCTION

The center of the Wanapitei impact structure is located ~34 km northeast of the city of Sudbury, in central Ontario, Canada (Fig. 1). The structure is interpreted to be ~7 to 8 km in diameter (Dence and Popelar, 1972) and has a K-Ar age of 37 ± 2 Ma (Winzer *et al.*, 1976). Dence and Popelar (1972) presented topographical, geophysical and petrographical evidence for an impact origin of the structure. Topographical evidence of this includes the shape of the lake and the predominantly concentric pattern of smaller lakes and streams around and within 5 km of Wanapitei Lake. This concentric pattern is also seen in joint patterns around the lake (Dressler, 1982). Geophysical indication for an impact origin is a local, more or less circular gravity depression of ~15 mgal over the circular, northern part of the lake. A horizontal gradient of >4 mgal/km outward from the center suggests a superficial mass deficiency with a circular plan (Dence and Popelar, 1972). Petrographic evidence for an impact origin is observed in boulders and pebbles of strongly shock metamorphosed rocks and suevitic breccia, found at a few locations south of the lake (Fig. 1; Dence and Popelar, 1972; Dence *et al.*, 1974; Grieve and Ber, 1994). The rounded boulders and pebbles have been transported south- to south-southwestward by the last Pleistocene glaciation event and had been scoured either from the bottom of the lake and/or from an ejecta blanket from around the impact structure. They make up less than five percent of the Pleistocene till. To date, no shock metamorphosed rocks unequivocally related to the Wanapitei impact structure have been found in place. Shatter cones have been noted in a few places on the shore and on islands of the lake. Planar deformation features in quartz have been observed in bedrock at three locations, on a tiny island in southwestern Wanapitei Lake, and in two places near the shores of southern Wanapitei Lake (Fig. 1). However, both the shatter cones and the microscopic shock metamorphic features were noted outside the assumed Wanapitei structure and, therefore, are related to the 1.85 Ga

old Sudbury impact structure within which the Wanapitei structure is located. The western shore of Wanapitei Lake is only ~3 km east of the Sudbury Igneous Complex (Fig. 1).

Target rocks consisted mainly of metasedimentary rocks of the Early Proterozoic Huronian Supergroup, Nipissing gabbroic intrusions associated with minor granophyre, granodiorite, granitic rocks and minor Archean granitic and gneissic rocks (Fig. 1). The Huronian metasediments are mainly arkosic arenites, wackes, conglomerates and very minor carbonate rocks. The wacke units, especially those of the 2700 m thick, glacial Gowganda Formation (Dressler, 1982) commonly contain pebbles (see legend of Fig. 1). Clasts derived from the Huronian sequence and the Nipissing intrusive rocks are common in the suevitic breccia boulders and pebbles. Archean granite clasts are very scarce. These clasts were subjected to all stages of shock metamorphism up to melting (~50–80 GPa). Wolf *et al.* (1980) inferred an admixture of >1% chondritic material in Wanapitei impact glass. This result has been substantiated by Evans *et al.* (1993), who analyzed the same glasses for Pt group element abundances. Grieve and Ber (1994) described a variety of shocked Wanapitei lithologies and provided a mixing model for an impact melt involving mainly metasedimentary target rocks. Dence *et al.* (1974) documented coesite in a vesicular, glass-rich quartzite boulder.

The objective of our investigation is a detailed description and analysis of a peculiar inclusion-bearing boulder whose components record similar degrees of shock-vitrification. The rock is a strongly shocked metasedimentary rock (*i.e.*, a pebbly, arkosic wacke) that originally and prior to the shock event contained various metasedimentary and crystalline rocks as clasts. The rock is not an inclusion-bearing impact melt derived through melting and homogenization of a large volume of target rocks. In comparison with some recent investigations on glasses of the Ries structure impact (Engelhardt *et al.*, 1995), we attempt to estimate the postdeposition annealing temperature of the investigated sample.

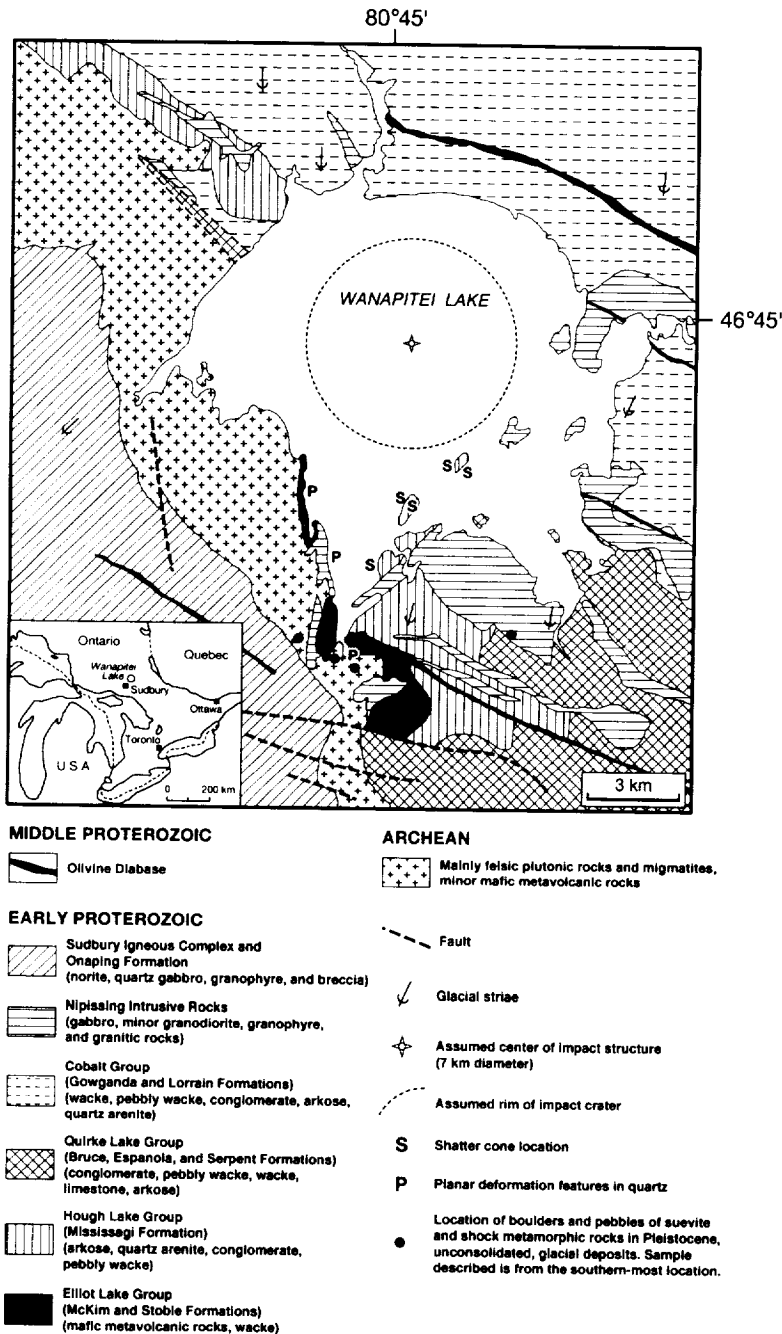


FIG. 1. General geology of the Wanapitei Lake area (after Dressler, 1982) showing the approximate size of the impact structure and the locations where suevite and shock metamorphosed lithologies were found in the unconsolidated, Pleistocene deposits south of the lake. Crater size estimate is based mainly on gravity (Dence and Popelar, 1972).

PETROGRAPHY AND GEOCHEMISTRY

The investigated boulder is 11.0 cm × 12.5 cm and exhibits six clasts A–E (Fig. 2, upper) and F (Fig. 2, lower, on back side of sample) embedded in a gray matrix. Between clasts A and C lies a small, stretched out clast E. The boulder matrix is fine grained with a macroscopic texture similar to common arkosic wackes of various units of the Huronian Supergroup (Fig. 3), for example the Mississagi, Serpent or Gowganda formations (Dressler, 1982). It is also

similar to a coesite-bearing, strongly shocked Wanapitei quartzite sample described by Dence *et al.* (1974). All clasts in our sample are fine grained and range from 1.5 cm to ~6.5 cm in length. Clast B is black, all others are gray. Clast A has a somewhat fluidal texture; clast B has a pumicelike, fluidal texture; all other clasts macroscopically are nonfluidal. Clast F (Fig. 2, lower) is rounded. All components of the sample, except clasts C and D, contain macroscopically visible amygdules and vesicles. These are spherical and very rarely ovoid, which are similar to the large vesicles in the host boulder matrix (Fig. 2, upper). Contacts between the boulder matrix and the various clasts are relatively sharp, with the exception of clasts C and E which have diffuse contacts with the boulder matrix. Clasts C and E have not been investigated here in detail.

Petrographic observations indicate that the boulder matrix and clasts are largely vitrified and exhibit various degrees of fluidization, vesiculation, and devitrification. The glass of the boulder matrix (Fig. 4), in most parts of the sample, is strongly devitrified. However, perlitic fractures are still recognizable in places. In portions of the specimen, especially near inclusions, the glass is fluidal. It is very similar to the glass of the clasts (*i.e.*, it is colorless and clear), containing fine microlites, relic quartz grains, amygdules, lined vesicles, and minor opaque minerals. Glass of the black clast A is brownish in plane-polarized light.

We analyzed glasses of boulder matrix and individual clasts with a defocused (~15 μm) electron beam, avoiding microlite- and relic mineral clast-bearing glass domains (Table 1). We found distinct differences in composition of the various glasses. For example, SiO₂ ranges from a low of 64.8% in clast F to 71.8% in clast A, while Al₂O₃ has a range from ~12.4% (clast A) to 18.85% (clast F). Near quartz grains and in small glass bodies within quartz grains, the silica content of the glasses increases considerably, accompanied by an slight increase in K₂O and a decrease in Al₂O₃ (Table 1 and Fig. 5).

The devitrification products in the boulder matrix and clasts are optically determined orthopyroxene microlites. No plagioclase or biotite has been observed. In clast F, we observed some tiny, stubby spinel and needles of mullite which, because of their shape, are believed to represent products of devitrification. The degree of devitrification is not the same in the various components of the investigated sample. In most of the boulder matrix (Fig. 4), tiny, light greenish, straight and curved microlites commonly form a dense, feltlike texture. In clast A, the orthopyroxene needles are light green and mostly straight (Fig. 6). Textures of clast F are similar to those of clast A. In the black clast B, the devitrification products are straight, branched or curved, and light green to brownish. Commonly they form dense, latticelike intergrown textures (Fig. 7). Clast D also exhibits light brownish, straight or curved microlites, while those in clast F are light greenish and straight, radiating needles (Fig. 8).

We carefully selected a number of pyroxene microlite needles in clasts and boulder matrix for microprobe analyses (Table 2). In many cases, the tiny needles are too thin to allow reliable analyses. We did not attempt to analyze microlites <2 μm wide, and we rejected all results that did not closely fit pyroxene stoichiometry.

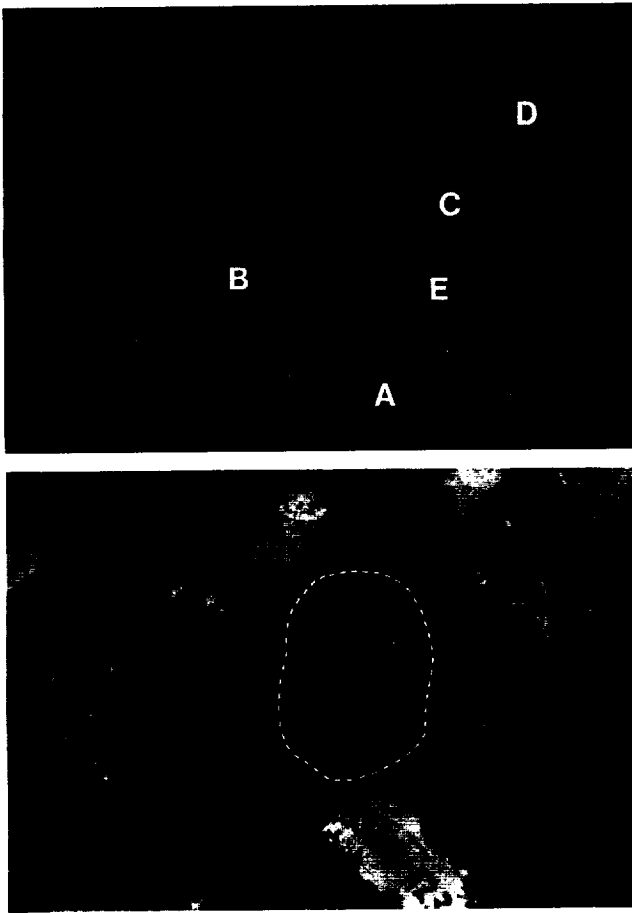


FIG. 2. Shock metamorphosed pebbly wacke of the Proterozoic Huronian Supergroup investigated in this paper. (upper) Clasts A–E show various degrees of vesiculation and fluidization. Sample is 11.0 × 12.5 cm. Note the large vesicles in the boulder matrix. (lower) Clast F is rounded, has a sharp contact with the boulder matrix and a diameter of ~3 cm.

We were successful in obtaining reliable results from only three of the five studied sample components, namely the boulder matrix and clasts B and D. Pyroxene microlites in clasts A and F are too small for reliable microprobe analysis. However, in clast F, we observed several stubby, up to 10 μm thick needles and stubby crystals different in appearance from the tiny pyroxenes. A total of six were analyzed, three of which have the composition of mullite; the three others are alumina-rich spinels with a Mg/Fe ratio indicative of pleonaste (Table 2). Both mullite and spinel occur isolated from each other and the pyroxene microlites. No feldspar or biotite microlites were detected with the light microscope or the electron microprobe. There appears to be no correlation between the compositions of the pyroxene microlites and that of the glasses of the various sample components.

The only relic original minerals within the microlitic impact glass of the boulder matrix and all clasts are quartz and minor opaque minerals. The modal content of relic quartz grains in the boulder matrix is ~30%. In clasts A, B, D, and F, we observed 50, 10–15, 45–55, and 25–35% quartz, respectively, reflecting the original, pre-shock quartz content. In the boulder matrix, two types of quartz grains have been observed. One type is clear and translucent; the other is brownish and semitranslucent. The translucent grains are angular to

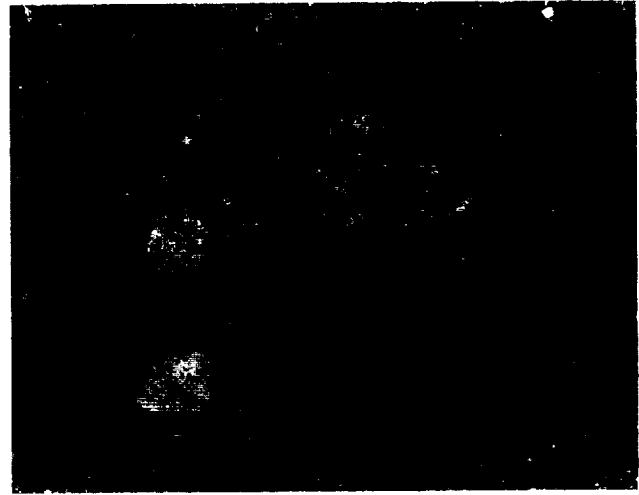


FIG. 3. Unshocked, pebbly wacke of the Huronian Supergroup believed to be similar to the progenitor of the sample investigated here. Similar rocks are common in the areas around Wanapitei Lake. Photograph courtesy of W. Meyer, Sudbury, Ontario.

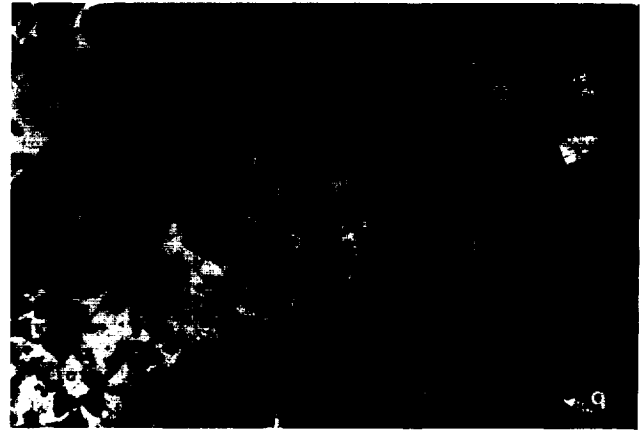


FIG. 4. Plane-polarized light image of strongly shocked boulder matrix consisting of feltlike, strongly devitrified glass, relicts of brownish, semitranslucent quartz grains (Q) and smectite filled amygdules (S). The devitrification is not homogeneous across the sample, and perlitic fractures are not present in this view of the boulder matrix. Smectite is color-zoned and exhibits radial shrinkage cracks. Small, translucent quartz grains (q) are also present. Most of them exhibit ballen structures. Length of photograph is 2.6 mm.

subrounded, and commonly embayed, droplike, or fluidally stretched (Fig. 9, upper), and exhibit "ballen" structures (Stähle, 1972; Carstens, 1975). The translucent ballen structures exhibit very fine-grained, flecky or fibrous recrystallization of quartz. The brownish, semitranslucent quartz grains are also angular to subrounded, but scarcely embayed and nowhere fluidally stretched. Many of them, here and in the other components of the studied sample, also exhibit ballen structures. The distinct ballen or small groups of ballen in one quartz grain show optical orientation different from each other or fine-grained flecky recrystallization. Both types of ballen-structured quartz grains may contain small round glass "inclusions" that in places contain microlites (Fig. 9, lower), or larger glass bodies (Figs. 5). The small "inclusions" may very well represent embayments of glass into the quartz grains. The quartz grains in the clasts commonly are brownish and many are ballen-structured. Some ballen-structured quartz in clast B has glass "inclusions" as noted in the

TABLE 1. Microprobe analyses of glasses.

n	Boulder Matrix						Clast A		Clast B		Clast D		Clast F	
	(1) Aver- age	STDEV	(2) Aver- age	STDEV	(3) Aver- age	STDEV	Aver- age	STDEV	Aver- age	STDEV	Aver- age	STDEV	Aver- age	STDEV
	12		4		9		6		6		4		6	
SiO ₂	66.18	2.48	75.15	0.71	74.72	1.18	71.77	1.96	69.58	1.68	68.49	1.69	64.76	1.19
TiO ₂	0.35	0.18	0.42	0.34	0.25	0.28	0.10	0.05	0.39	0.20	0.12	0.05	0.19	0.09
Al ₂ O ₃	16.41	1.66	11.38	0.76	11.92	1.03	12.36	0.99	15.97	1.20	16.90	1.05	18.85	1.61
FeO	3.40	3.03	2.09	0.37	1.36	0.38	1.61	0.24	2.38	1.10	1.35	0.24	2.56	0.54
MnO	0.02	0.02	0.04	0.06	0.02	0.02	0.04	0.03	*		0.01	0.01	0.04	0.03
MgO	1.57	0.37	1.11	0.17	0.86	0.16	0.86	0.15	0.64	0.67	0.57	0.19	1.31	0.22
CaO	0.86	0.19	0.39	0.12	0.41	0.07	2.61	0.47	1.38	0.54	0.44	0.10	0.31	0.09
Na ₂ O	3.11	0.92	2.67	0.58	2.44	0.80	3.24	0.41	3.98	2.13	2.62	0.22	2.61	0.29
K ₂ O	3.17	0.99	3.92	0.45	4.12	0.58	2.80	0.06	2.49	1.07	4.63	0.43	5.62	0.54
P ₂ O ₅	0.09	0.05	0.05	0.02	0.12	0.06	0.02	0.02	0.30	0.12	0.07	0.06	0.04	0.04
Cr ₂ O ₃	0.02	0.05	*		0.02	0.01	0.01	0.02	*		0.01	0.01	0.01	0.01
Total	95.18		97.22		96.24		95.42		97.11		95.21		96.30	

(1) Boulder matrix glass. (2) Boulder matrix glass at contact with quartz grains. (3) Glass within ballen quartz.

STDEV = Standard deviation. n = Number of analyses. FeO = Fe total. *Below detection limit.

Analyses performed with defocused (~15 μm) electron beam (15 kV; 20 nA).

boulder matrix quartz. Clast B is also the only component of the investigated sample that contains minor diaplectic quartz; however, based on thin section work, all relic quartz has reduced refractive indices and anomalous, low birefringence. The glass of both the "inclusions" and of the larger bodies in the quartz grains of the boulder matrix is somewhat richer in SiO₂ and K₂O and poorer in Al₂O₃ than the main mass of the boulder matrix glass (Table 1, Fig. 5).

Within the larger, ballen-structured quartz grain of Fig. 5, the glass bodies exhibit faintly visible, semicircular heterogeneities which we identified by microprobe as essentially pure silica. These semicircles have the shape of ballen rims.

Under the microscope, both the clasts and the boulder matrix of our sample exhibit amygdules and lined vesicles. The boulder matrix has some large empty vesicles (Fig. 2, upper). Clast D also has

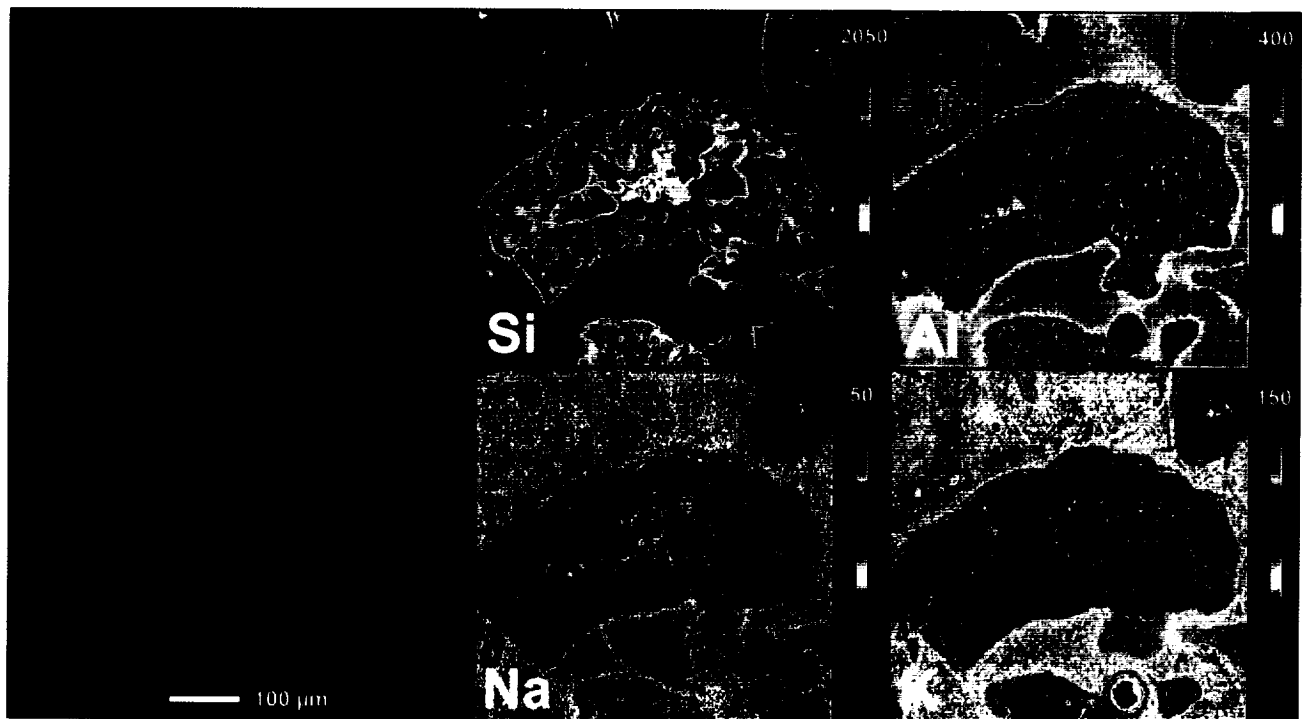


FIG. 5. Backscattered electron (BSE) image and element maps showing ballen-structured quartz grains in glass of boulder matrix. Within the interior of the large, semi-translucent quartz grain are relic ballen rims of essentially pure silica. Note perlitic cracks and orthopyroxene microlites (lower right of BSE image) in matrix glass. Vesicles are lined with smectite. Distinct compositional gradients are apparent at the boundaries between quartz grains and the adjacent glass matrix. With the exception of K, all other elements analyzed show monotonically increasing concentrations with increasing distance from the quartz contact. In contrast, K is significantly enriched near the contact, indicating "uphill" diffusion against the silica concentration gradient. Intensity scales show absolute counts obtained by wavelength-dispersive x-ray scanning at a rate of 100 milliseconds per pixel. The x-ray maps were scanned at a resolution of 512 × 512 pixels.



FIG. 6. Plane-polarized light image of weakly devitrified glass of clast A containing relicts of quartz grains (Q) and amygdules completely or partially filled with smectite (S). Some of the relic, subangular to rounded quartz grains, faintly exhibit ballen structures. The large vesicle is lined with light yellowish smectite that has radial shrinkage cracks. Length of photograph is 2.6 mm.

irregularly shaped, lined cavities (Fig. 10). The material filling amygdules or lining vesicles and cavities is yellow, brown to dark brown. Color zoning is common, with the center of amygdules commonly exhibiting the darkest colors. Radial shrinking cracks were noted. We have analyzed the material filling or lining the vesicles and irregularly shaped cavities with a defocused ($15\ \mu\text{m}$) electron beam. Thin section polishing commonly destroyed smectite vesicle fillings and not everywhere were we successful in obtaining a satisfactory number of microprobe analyses. The results obtained (Table 3), however, compare well with published analyses of smectites and indicate a heterogeneous character of the smectites. The low totals reflect their volatile content. Some of the results indicate a weak correlation between smectite composition and glass (*i.e.*, original rock composition). Iron and Mg are both highest in the smectite and glass of clast B. Iron is lowest in both smectite and glass of clast D. Other elements, however, do not correlate in any obvious way (Table 3). We believe that those target rock clasts with higher smectite content probably contained more water-bearing mineral phases than those with less smectite in the mode. The Proterozoic metasandstones of the Wanapitei Lake area, for example, modally contain ~4 to 60% cement consisting of water-bearing phases such as biotite, sericite, and chlorite and, in places, minor carbonate and opaque minerals (Dressler, 1982). Smectite probably was deposited in the vesicles immediately after vitrification of the sample.

The microscopic texture of portions of the boulder matrix is reminiscent of a metasedimentary rock. Clast A contains ~50% relic quartz grains and, as clast F, shows a texture also reminiscent of a metasediment. Clast B has no original texture preserved. Clast D, however, has a well preserved sedimentary texture with subrounded quartz grains set in glass (Fig. 11, upper and lower). On the basis of petrographic work on rocks from around the Wanapitei impact structure (Dressler, 1982), the glass in clast D and much of the glass in the other components of our sample is interpreted to represent mainly melting of a greenschist facies mineral cement of fine-grained sericite, chlorite, epidote, quartz and plagioclase.

DISCUSSION

The peculiar, shock metamorphosed rock petrographically and geochemically analyzed here represents either a homogenized, clast-bearing impact melt derived through melting of various target rocks



FIG. 7. Plane-polarized light image of branched microlites of orthopyroxene in clast B. Note large vesicle. Not all of clast B is that strongly devitrified. Length of photograph is 0.65 mm.

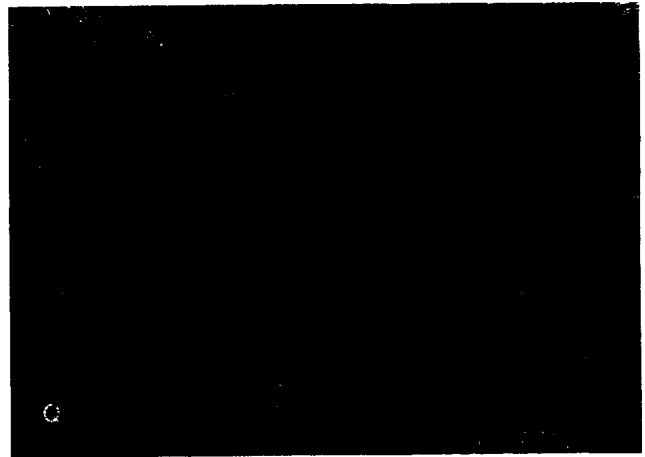


FIG. 8. Plane-polarized light image of radiating microlites of orthopyroxene in clast F. Brownish, semitranslucent quartz grains (Q) with ballen structures. Length of photograph is 0.65 mm.

or a strongly shocked, pebbly, arkosic wacke that originally and prior to the shock event and incipient melting contained a number of metasedimentary and igneous rock clasts. On the basis of our observations, we argue for the second interpretation; provide an estimate of the shock pressure experienced by the sample that led to partial melting and, in comparison with some recent investigations on the Ries structure impact glasses (Engelhardt *et al.*, 1995), estimate the postdeposition, annealing temperature of the specimen.

Macroscopically, our sample is not dissimilar to pebbly wacke (Fig. 3), pebbly arkoses or paraconglomerates of various formation of the Huronian Supergroup common in the target rocks of the Wanapitei structure (legend of Fig. 1; Dressler, 1982). The sample matrix resembles a Wanapitei impact rock described by Dence *et al.* (1974) as a coesite-bearing, vesicular quartzite.

The microscopic textures of clasts A, D, F, and of portions of the boulder matrix are reminiscent of that of metasedimentary rocks. In all the clasts and the boulder matrix, quartz and some minor opaque grains are the only minerals that were not completely shocked. Many quartz grains have retained rounded or subrounded shapes of probable clastic origin. In the boulder matrix, however,

TABLE 2. Microprobe analyses of microlites.

n	Pyroxene					Mullite		Spinel	
	Boulder Matrix Average 2	Clast B		Clast D		Clast F*			
	Average	STDEV	Average	STDEV	Average	STDEV	Average	STDEV	
	8	6	3	3					
SiO ₂	50.64	45.64	1.25	48.61	1.01	26.85	1.11	0.13	0.05
TiO ₂	0.15	0.27	0.16	0.10	0.05	0.84	0.42	0.16	0.09
Al ₂ O ₃	10.85	12.18	1.45	14.19	1.16	68.25	2.88	59.58	0.46
FeO	18.19	21.38	2.29	9.67	0.43	1.85	0.69	21.83	0.30
MnO	0.16	0.19	0.05	0.07	0.03	0.01		0.01	
MgO	19.03	18.48	1.67	26.54	0.51	0.41	0.41	17.76	0.44
CaO	0.55	0.30	0.18	0.06	0.01	0.03	0.02	0.01	0.01
Na ₂ O	0.13	0.04	0.02	0.02	0.01	0.27	0.07	0.02	
K ₂ O	0.22	0.03	0.03	0.06	0.04	0.18	0.09	0.04	0.02
P ₂ O ₅	0.03	0.04	0.04	0.07	0.04	0.09	0.14		
Cr ₂ O ₃	0.13	0.14	0.10	0.11	0.06	0.15	0.08	0.79	0.38
Total	100.08	98.69		99.50		98.93		100.32	
Si	1.837	1.704	0.030	1.710	0.036				
Al	0.163	0.307	0.028	0.290	0.036				
Al	0.300	0.256	0.049	0.299	0.021				
Fe ⁺⁺	0.552	0.671	0.075	0.284	0.013				
Mg	1.028	1.039	0.079	1.391	0.026				
Ca	0.021	0.013	0.006	0.002	0.001				
Na	0.009	0.002	0.001	0.001	0.001				
K	0.010	0.002	0.001	0.003	0.001				
Ti	0.004	0.008	0.004	0.003	0.001				
Mn	0.005	0.006	0.001	0.002	0.001				
P	0.001	0.002	0.001	0.002	0.001				
Cr	0.004	0.005	0.003	0.003	0.002				
Sum	3.934	4.015		3.990					
Z	2.000	2.000		2.000					
X	1.934	2.015		1.990					

n = Number of analyses. FeO = Fe total. STDEV = Standard deviation.

*Fragments F and A contain pyroxene microlites too small for microprobe analysis.

Analyses performed with focused electron beam (~1 μm; 15 kV; 4 nA).

few quartz grains have elongate, fluidal shapes that are indicative of viscous flow. Vesicles plus amygdules make up ~1 to 20% of the various components. The boulder matrix has the lowest vesicle plus amygdule abundance (Table 4). Vesicles are known to exist in highly shock metamorphosed rocks and have also been described by Dence *et al.* (1974) from their partially melted, coesite-bearing Wanapitei quartzite sample. The extent of melting and vitrification of the boulder matrix and most of the described clasts appears to be similar to that observed by Kieffer (1971) in her class 4 and class 5 shocked rocks. In her class 4 rocks, for example, remnant quartz grains and clasts appear to float in vesicular glass which is similar to what we observe in our sample. Our macroscopic and microscopic observations, therefore, are consistent with our interpretation of the investigated sample as a shock metamorphosed pebbly wacke.

All sample components contain glass. Glasses are chemically heterogeneous resulting in high standard deviations (Table 1). This heterogeneity is believed to reflect the originally heterogeneous character of the vitrified rocks and the less than perfect rock vitrification and very limited mixing of the glasses. Boulder matrix glass, in general, has considerably lower silica and potash and higher alumina contents than boulder matrix glasses in embayments of, or very close to quartz grains, or where glass is included in ballen-structured quartz (Fig. 5). We believe that high viscosity of the silica-rich glasses and stress conditions have not been conducive to

mixing of the incipient melts, resulting in the preservation of chemical heterogeneities. The low analytical totals (~95 to 97%) reflect the volatile content of the glass. Although glasses may undergo secondary hydration, these are clear and uncolored. The vesicularity of the glasses, however, is a reflection of the original volatile content. Our chemical and petrographical observations suggest that preshock high volatile content may be conducive to the formation of many, relatively small vesicles and amygdules (clasts of the analyzed sample) whereas low volatile content results in larger but fewer vesicles and amygdules (boulder matrix) substantiating the results of Kieffer *et al.* (1976). Our glass compositions are not dissimilar to the glass compositions of the coesite-bearing, vesicular quartzite analyzed by Dence *et al.* (1974). The abundance of nonrecrystallized glass in both the clasts and boulder matrix is indicative of rapid cooling. The sample, therefore, is not derived from a thick melt sheet from within the crater cavity. As such it would have developed a geochemically probably homogeneous, crystalline matrix possibly with typical reaction coronas of pyroxene and/or biotite around quartz grains as described from melts of other impact structures such as Manicouagan (Floran *et al.*, 1978). However, minor element transport in the supercooling glass of our sample had occurred as suggested by Fig. 5.

Pyroxene microlites in our sample are alumina-rich which is a characteristic of pyroxenes in supercooled lunar and terrestrial impact

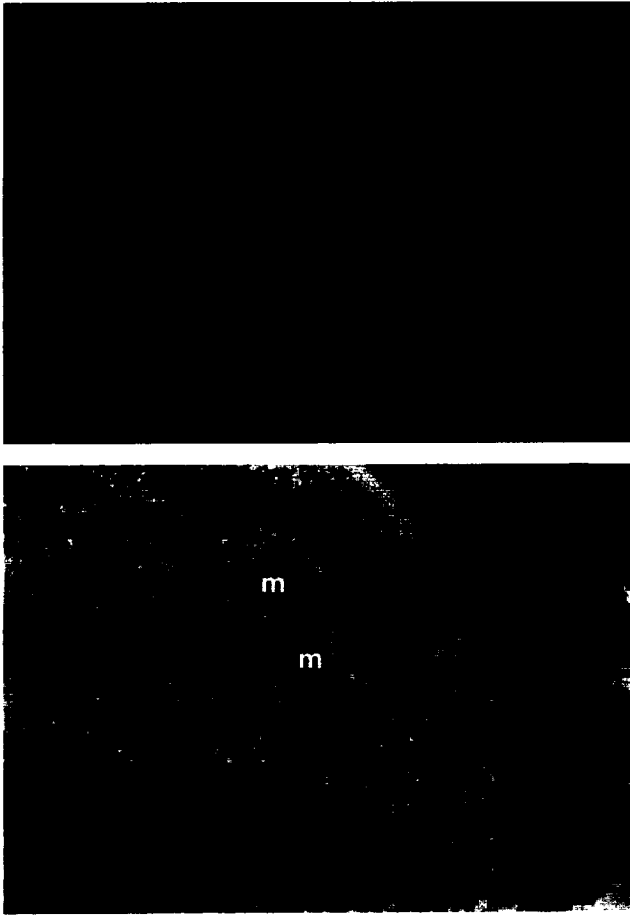


FIG. 9. (upper) Plane-polarized light image of droplike, translucent quartz grains exhibiting ballen structures, embedded in glass of boulder matrix. Alignment of elongate quartz is indicative of viscous flowage in this portion of the boulder matrix. Length of photograph is 0.65 mm. (lower) Plane-polarized light image of part of ballen-structured quartz grain with droplike inclusions of microlite-bearing glass (m) set in strongly devitrified glass in boulder matrix (cf., Fig. 5). Inclusions may represent embayments of matrix glass into lechatelierite prior to vitrification. Note smectite-lined vesicle and semitranslucent, birefringent quartz grains devoid of ballen structures and planar deformation features. Boulder matrix glass. Length of photograph is 0.65 mm.

melts (Engelhardt *et al.*, 1989). Apparently, there is no correlation between pyroxene microlite composition and the composition of the enclosing glass (Tables 1 and 2). This is believed to be also a result of rapid disequilibrium cooling. All the analyzed sample components experienced equal high-pressure shock melting and subsequent supercooling.

The chemical bulk composition of the clasts and the rock boulder matrix may allow us to classify the sample components as either sedimentary or igneous, and in consequence, even to assign our pebbly wacke to a specific formation of the Huronian Supergroup. To arrive at an approximate whole rock chemical composition of the unshocked boulder matrix and clasts, the modal percentages of unmelted, relic quartz (in all cases feldspar and sedimentary cement supporting the quartz grains melted preferentially) were proportionally added to the glass analyses. We assume that no components were introduced or removed postimpact (Table 4). The high silica contents of the boulder matrix and of clasts A and D are charac-



FIG. 10. Plane-polarized light image of irregularly shaped vesicles lined with smectite in clast D. Length of photograph is 2.6 mm.

teristic of quartz-rich, sedimentary rocks. This classification is supported by their texture. Clast F has a chemical composition of a metasediment or of an igneous rock, but as mentioned above, has a relic sedimentary texture. Clast B, as clast F, has a chemical composition of a metasedimentary or igneous rock and has no rock texture preserved. The volatile-free analyses are all silica-rich, especially those of the boulder matrix and clasts A and D, supporting our interpretation that most clasts and the boulder matrix represent metasedimentary rocks. On the basis of our knowledge of the regional geology of the Wanapitei area (Dressler, 1982), we tentatively assign our analyzed pebbly wacke to the Serpent Formation. Paraconglomerates and pebbly wackes of this formation in the Wanapitei Lake area are characterized by clasts derived mainly from metasedimentary rocks. In contrast, similar rocks of other formations contain mainly clasts of igneous rocks.

Shock metamorphic features observed in Wanapitei impact rocks are planar deformation features (PDFs) in quartz and feldspars, quartz mosaicism, mineral shock isotropization, and rock and mineral melting (Dence and Popelar, 1972; Dressler, 1982; Grieve and Ber, 1994). Dence *et al.* (1974) documented the presence of coesite in a vesicular, Huronian quartzite boulder. In the sample studied here, we have noted only one small quartz grain with two sets of PDFs, and only in clast B did we note a few grains of shock-isotropic, nonrecrystallized, diaplectic quartz. The development of PDFs appears to be depressed in some strongly shocked (meta)sedimentary rocks, even in rocks that contain coesite, diaplectic glass and glass as described by Kieffer (1971) who noted <5% quartz grains with PDFs in shocked Coconino quartz sandstone of Meteor Crater that contains 8 to 10% glass. On the basis of observations from the Sudbury Structure (Dressler, unpublished data), the development of PDFs in quartz of metasedimentary rocks, in general, may be depressed compared to that in crystalline target rocks. This may be an effect of initial porosity. However, the Proterozoic metasedimentary target rocks at Lake Wanapitei and in places around the Sudbury Igneous Complex have no microscopically detectable porosity. We therefore speculate that in common metasedimentary rocks the compressibility differences of "competent" quartz grains and "incompetent" greenschist facies cement of chlorite, sericite, and saussuritized plagioclase may have had the same effect as rock porosity in inhibiting PDF development (and—possibly—development of large impact melt volumes). Besides the observations of very scarce PDFs and diaplectic quartz, evidence for an origin by shock of our sample is the presence of impact glass and

TABLE 3. Microprobe analyses of amygdule fillings (smectite).

n	Boulder Matrix		Clast A		Clast B		Clast D		Clast F	
	Average	STDEV	Average	STDEV	Average	STDEV	Average	STDEV	Average	STDEV
	2	2	6	6	2	2	11	11	20	20
SiO ₂	52.79	3.41	57.02	1.69	63.59	0.04	51.16	3.60	55.32	1.09
TiO ₂	0.45	0.00	0.24	0.07	0.30	0.02	0.08	0.05	0.27	0.16
Al ₂ O ₃	14.78	0.86	19.41	1.22	17.19	0.36	15.14	1.76	18.19	0.88
FeO	2.42	0.21	2.71	0.24	3.16	0.18	2.05	0.13	2.33	0.15
MnO	0.03	0.04	0.09	0.03	0.03	0.03	0.04	0.03	0.04	0.03
MgO	3.78	0.08	3.68	0.51	4.18	0.00	3.53	0.27	3.35	0.16
CaO	2.20	0.01	1.74	0.21	2.21	0.21	2.07	0.22	1.76	0.20
Na ₂ O	0.21	0.08	0.04	0.04	0.09	0.04	0.04	0.03	0.05	0.02
K ₂ O	0.59	0.08	0.13	0.02	0.30	0.09	0.23	0.09	0.28	0.09
P ₂ O ₅	0.06	0.07	0.05	0.02	*		0.02	0.01	0.06	0.09
Total	77.31		85.11		91.05		74.36		81.65	

n = Number of analyses. Low totals reflect volatile content. STDEV = Standard deviation. FeO = Fe total. *Below detection limit. Analyses performed with a defocused electron beam (15 μ m; 15 kV, 20 nA).

quartz grains with ballen structures (Fig. 9, upper and lower). Ballen quartz has been interpreted to represent pseudomorphs after cristobalite which, in turn, is thought to have replaced lechatelierite, formed by shock (Carstens, 1975) or represent recrystallized diaplectic glass or liquid-state glass that underwent transition to cristobalite and α -quartz (Bischoff and Stöffler, 1981; 1984). The droplike shape of some of the translucent ballen quartz grains supports the interpretation of Carstens (1975). We have noted some peculiar ballen-structured, brownish quartz grains that contains relatively large bodies of glass in their interior. In one of these glassy interiors (Fig. 5), we observed ghostlike, relic ballen rims consisting of silica. The texture is suggestive of incipient melting and assimilation of ballen quartz by the melt. The configuration of melt within the ballen-structured quartz grain in Fig. 5 is interpreted as being the result of a 3-D effect. The preservation of portions of the ballen rims in the melt may indicate that the rims consisted, or still consist of a silica phase different from, and more resistant to melting than the ballen itself. The brownish, ballen-structured, semitranslucent quartz grains may represent pseudomorphs after diaplectic quartz glass rather than lechatelierite. The diaplectic quartz reverted to quartz upon cooling, supporting one of the above interpretations of Bischoff and Stöffler (1981, 1984). The lack of fluidal, droplike shapes of the brownish, semitranslucent quartz supports this view. Bischoff and Stöffler (1984), in a study of impact rocks from Lappajärvi structure, Finland, assigned specific shock pressures to various optical characteristics of the ballen-structured quartz. According to them, incipient formation of ballen structure is characteristic of a shock pressure range of ~10–30 GPa, optical homogeneous ballen indicate ~30–45 GPa, and ballen with different optical orientation in one grain and intra-ballen recrystallization suggest shock ranges of ~45–55 GPa. On the basis of our observation and the comparison with the results of Bischoff and Stöffler (1984), ballen-structured quartz in our sample was subjected to these high, ~45–55 GPa shock pressures. The absence of feldspar and the observation of fluidally shaped quartz glass bodies are evidence that our sample experienced temperatures of >1700 °C, (*i.e.*, above the liquidus temperature of any plagioclase) and high enough to account for the formation of lechatelierite, which according to Carstens (1975) is the precursor of ballen quartz. However, not all quartz in our sample experienced melting.

All the clasts and the boulder matrix of our Wanapitei impact rock specimen have ballen-structured quartz and impact glass. Shock melting occurs when rocks are subjected to peak pressures of

>50–60 GPa. Based on our observation of ballen structures and their optical orientation and the presence of impact glass, all our sample experienced the same shock pressure. Impact melts, however, commonly contain clasts that were subjected to various degrees of shock metamorphism. Bischoff and Stöffler (1984), for example, describe shock features in clasts of the Lappajärvi structure that had been subjected to peak pressures ranging from <10 to ~55 GPa.

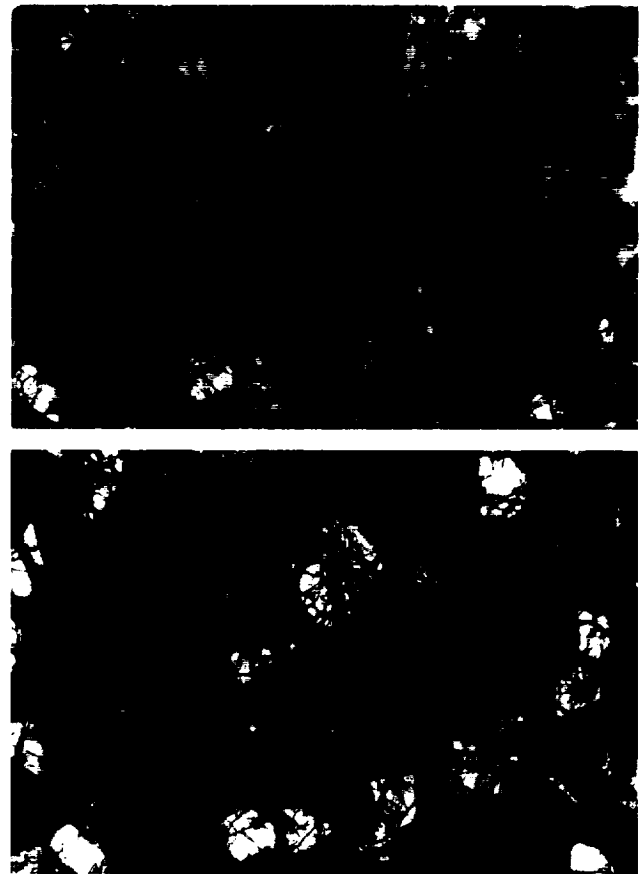


FIG. 11. Relict quartz grains in strongly devitrified glass of clast D seen in (upper) plane polarized light and (lower) with crossed polarizers. Sedimentary cement of this sandstone clast is vitrified while quartz grains are not. Length of photograph is 2.6 mm.

TABLE 4. Whole rock compositions of boulder matrix and fragments.[†]

	Boulder Matrix		Clast A		Clast B		Clast D		Clast F	
SiO ₂	79.50	82.14	81.17	83.74	74.11	76.05	86.61	88.42	75.33	77.33
TiO ₂	0.21	0.22	0.07	0.07	0.33	0.34	0.05	0.06	0.13	0.13
Al ₂ O ₃	9.76	10.08	8.24	8.50	13.56	13.91	7.18	7.33	13.20	13.55
FeO	1.62	1.67	1.07	1.10	2.02	2.07	0.57	0.58	1.79	1.84
MnO	0.01	0.01	0.03	0.03	*		0.01	0.01	0.03	0.03
MgO	0.81	0.84	0.57	0.59	0.54	0.55	0.24	0.25	0.92	0.94
CaO	0.46	0.48	1.74	1.80	1.17	1.20	0.19	0.20	0.21	0.22
Na ₂ O	1.88	1.94	2.16	2.23	3.37	3.46	1.11	1.14	1.83	1.88
K ₂ O	2.46	2.54	1.86	1.92	2.11	2.16	1.97	1.98	3.93	4.04
P ₂ O ₅	0.07	0.07	0.01	0.01	0.25	0.26	0.03	0.03	0.03	0.03
Cr ₂ O ₃	0.01	0.01	0.01	0.01	0.00	0.00	0.00	0.00	0.01	0.01
Total	96.79	100.00	96.93	100.00	97.46	100.00	97.96	100.00	97.41	100.00
V+A	0.80%		19.80%		12.60%		16.40%		8.60%	

[†]See text; right column volatile-free. FeO = Fe total. *Below detection limit. V+A = Modal% of vesicles and amygdules in glass.

This is evidence that all components of our sample were subjected to the same high shock pressure probably together as pebbly arkosic wacke. If one or more of the clasts or the boulder matrix had experienced different shock pressures, we would have to interpret the boulder matrix of the investigated rock as an impact melt and not as a shock-vitrified wacke matrix.

We have shown that all components of the glassy Wanapitei impact rock boulder had been subjected to a peak shock pressures of ~50–60 GPa and to a temperature of >1700 °C. Microscopic textures are indicative of very rapid cooling. Very similar textures have been observed in glasses from other terrestrial impact glasses, such as the Ries structure in Germany. It is known from the Ries structure that fallout suevite glass clasts were brittle when they landed, that is, they had cooled sufficiently during the ejection process from >1700 °C (ballen textures in quartz after lechatelierite and cristobalite) to under 750 °C. Engelhardt *et al.* (1995) have shown that the transformation temperature for synthetic glass of Ries melt composition is 680 °C (*i.e.*, the temperature at which a viscous, undercooled Ries melt transforms to brittle glass). They have further shown that this glass begins to deform plastically upon heating at 750 °C. The suevite was deposited above 580 °C, the Curie temperature of magnetite, because all Ries suevite deposits are characterized by a uniform remanent magnetization (Pohl and Angenheister, 1969). Therefore, the fallout suevite at the Ries was deposited at a temperature of between 580 °C and 750 °C. Nondevitrified glass in the Ries fallout suevite deposits occurs only in chilled zones of which the lower one is up to 2 m, the upper up to 10 m thick (Engelhardt *et al.*, 1995). Partially devitrified glasses occur ~1–2 m above the lower contact and to somewhat greater depth in the upper chilled zone. At the contacts themselves, the glasses are not devitrified. Glasses of the crater suevite at the Ries impact structure are, to a very large extent, strongly altered to montmorillonite and zeolites.

The analyzed Wanapitei sample was obtained from Pleistocene glacial float just south of the Wanapitei structure. Therefore, we do not know if it originally was deposited inside or outside the impact crater. On the basis of a comparison of the microscopic textures with those described from the Ries by Engelhardt *et al.* (1995), we can speculate that our sample was derived either from a thin melt body or from a chilled border of a relatively thick impact melt body of the crater interior or from a rapidly cooled suevitic breccia body, that is from within or from outside the crater. Only at these locations can textures as observed form and be preserved.

Engelhardt *et al.* (1995) also show that pyroxene microlites alone develop in devitrifying glass of Ries melt composition at specific temperatures and at lower pH₂O than plagioclase plus pyroxenes biotite plus plagioclase, or biotite plus plagioclase plus pyroxene. The Wanapitei sample studied here contains only pyroxenes as devitrification products, plus very minor mullite and spinel, and in part, has glass compositions (*e.g.*, clast F) not that different from Ries melt compositions. Wanapitei suevite glasses are vesicular and contain smectite. We therefore assume that the pH₂O possibly was not much different from that in common Ries melts. On the basis of our microscopical observations, cooling experienced by the Wanapitei specimen must have been similar to that of chilled, unaltered Ries glasses, and based on our findings and a comparison of our results with those of Engelhardt *et al.* (1995), we believe that the annealing temperature after deposition was somewhere between 650 °C and 800 °C for the sample studied here (Fig. 12). Stubby mullite and spinel microlite needles observed in clast F likely formed during devitrification. Synthetic mullite is formed in the porcelain industry at temperatures between ~1000 °C to 1600 °C (Tröger 1969). Spinel is common in high temperature regimes.

CONCLUDING REMARKS

Shock metamorphosed rocks and impact melts at Wanapitei Lake and other terrestrial impact structures are characterized by a wide range of textures and mineralogical and geochemical compositions reflecting target rocks and shock levels experienced by them. Quartz, arenites, wackes, pebbly wackes, and other sedimentary rocks of the Huronian Supergroup represent the bulk of the Wanapitei target rocks and make up a good proportion of the shock metamorphosed clasts in the Wanapitei suevitic breccia. Pebbly wackes, pebbly arkosic wackes and paraconglomerates make up a substantial proportion of the target stratigraphy. Our observation of ballen-structured quartz and impact glasses provides us with a shock pressure estimate experienced by the investigated sample of ~50–60 GPa (Stöffler, 1971; Bischoff and Stöffler, 1984; Stöffler and Langenhorst, 1994; and references therein). At this pressure, the sedimentary cement supporting quartz grains and some of the quartz grain themselves of both the clasts and the boulder matrix experienced shock melting as did other nonquartz rock forming components such as feldspars that probably were present in the sample investigated. Had this specimen been subjected to slightly higher shock pressures and stress facilitating mixing of the high-silica viscous

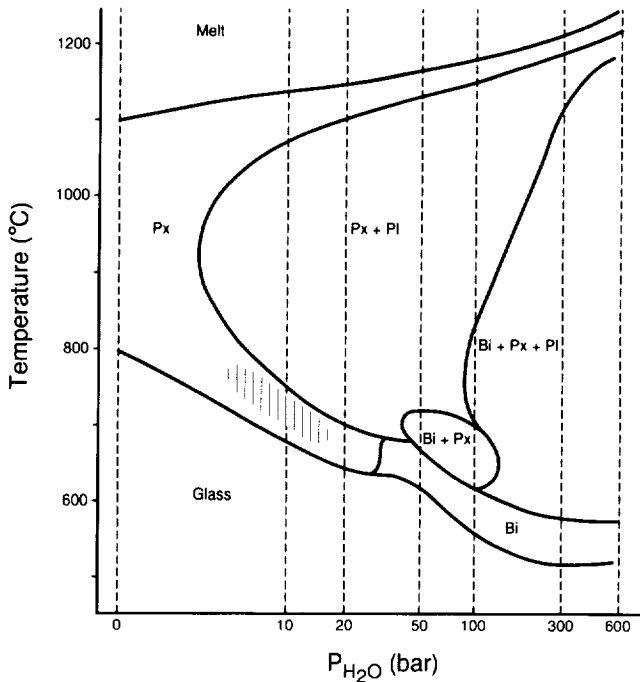


FIG. 12. Crystalline phases obtained by annealing vitreous Ries suevite glass for 10 h as a function of temperature and H_2O pressure (from Engelhardt et al., 1995). Hatched field may represent conditions under which all sample components investigated here devitrified.

melt, it would have been transformed into a homogeneous, high silica impact melt comparable to an average composition of all sample components. Relic quartz grains in the various glasses are practically devoid of planar deformation features (PDFs) and have low refractive indices and low birefringence. We speculate that rock textures and composition of the greenschist facies cement of the components of our sample possibly had the same effect as porosity of unmetamorphosed sedimentary rocks in depressing the development of PDFs and in inhibiting production of large melt volumes. Our rock textures are similar to those described from Kieffer's (1971) class 4 and 5 shocked Coconino sandstone of Meteor Crater, Arizona.

The sample investigated here is either an inclusion-bearing impact melt derived through melting of various target rocks or a strongly shock metamorphosed pebbly wacke which records the onset of shock melting. A number of our petrographical and geochemical observations by themselves do not unequivocally support either view. However, we have shown that degree of shock metamorphism and incipient melting in all components of our sample are very similar. The boulder matrix has textures and chemical composition similar to rocks classified as strongly shocked metasediments by other investigators. Taken together, our observations provide good evidence that the investigated sample is a strongly shock metamorphosed rock that originated from a rapidly cooled suevitic breccia deposit, either from within the Wanapitei impact crater or from an area around it.

Acknowledgments—We gratefully acknowledge the perceptive and instructive reviews of this paper by W. von Engelhardt and an anonymous reviewer. An early draft was reviewed by G. Graup and V. L. Sharpton. This is Lunar and Planetary Institute contribution 900.

Editorial handling: R. A. F. Grieve

REFERENCES

- BISCHOFF A. AND STÖFFLER D. (1981) Thermal metamorphism of feldspar clasts in impact melt rocks from Lappajärvi crater, Finland (abstract). *Lunar Planet. Sci.* **12**, 77–79.
- BISCHOFF A. AND STÖFFLER D. (1984) Chemical and structural changes induced by thermal annealing of shocked feldspar inclusions in impact melt rocks from Lappajärvi crater, Finland. *J. Geophys. Res. suppl.* **89**, 645–656.
- CARSTENS H. (1975) Thermal history of impact melt rocks in the Fennoscandian Shield. *Contrib. Mineral. Petrol.* **50**, 145–155.
- DENCE M. R. AND POPELAR J. (1972) Evidence for an impact origin for Lake Wanapitei, Ontario. *Geol. Assoc. Can., Sp. Pap.* **10**, 117–124.
- DENCE M. R., ROBERTSON, P. B. AND WIRTHLIN, R. L. (1974) Coesite from the Lake Wanapitei crater, Ontario. *Earth Planet. Sci. Lett.* **22**, 118–122.
- DRESSLER B. O. (1982) Geology of the Wanapitei Lake area, District of Sudbury. *Ontario Geol. Surv. Rep.* **213**, 131 pp.
- ENGELHARDT W. V., ARNDT J., FECKER B. AND PANKAU H. G. (1995) Suevite breccia from the Ries crater, Germany: Origin, cooling history and devitrification of impact glasses. *Meteoritics* **30**, 279–293.
- ENGELHARDT W. V., ARNDT J., PANKAU H. G. AND WITZSCH A. (1989) Al-rich pyroxenes: Supercooled lunar basaltic and terrestrial impact melts (abstract). *Lunar Planet. Sci.* **20**, 266–267.
- EVANS N. J., GREGOIRE D. C., GRIEVE R. A. F., GOODFELLOW W. D. AND VEIZER J. (1993) Use of platinum-group elements for impactor identification: Terrestrial impact craters and the Cretaceous-Tertiary boundary. *Geochim. Cosmochim. Acta* **57**, 3737–3748.
- FLORAN R. J., GRIEVE R. A. F., PHINNEY W. C., WARNER J. L., SIMONDS C. H., BLANCHARD D. P. AND DENCE M. R. (1978) Manicouagan impact melt, Quebec, I. Stratigraphy, petrology and chemistry. *J. Geophys. Res.* **83**, 2737–2758.
- GRIEVE R. A. F. AND BER. J. (1994) Shocked lithologies at the Wanapitei impact structure, Ontario, Canada. *Meteoritics* **29**, 621–631.
- KIEFFER S. W. (1971) Shock metamorphism of the Coconino sandstone at Meteor crater, Arizona. *J. Geophys. Res.* **76**, 5449–5473.
- KIEFFER S. W., PHAKEY P. P. AND CHRISTIE J. M. (1976) Shock processes in porous quartzite: Transmission electron microscope observations and theory. *Contrib. Mineral. Petrol.* **59**, 41–93.
- POHL J. AND ANGENHEISTER G. (1969) Anomalien der Erdmagnetfeldes und Magnetisierung der Gesteine im Nördlinger Ries. *Geologica Bavarica* **61**, 327–336.
- STÄHLE V. (1972) Gläser aus dem Suevit des Nördlinger Ries: Petrographische Untersuchungen und chemische Analysen mit der Elektronenstrahl-Mikrosonde. Inaug.-Dissert., University of Tübingen, Germany. 65 pp.
- STÖFFLER D. (1971) Progressive metamorphism and classification of shocked and brecciated crystalline rocks at impact craters. *J. Geophys. Res.* **76**, 5541–5551.
- STÖFFLER D. AND LANGENHORST F. (1994) Shock metamorphism of quartz in nature and experiment: I. Basic observation and theory. *Meteoritics* **29**, 155–181.
- TRÖGER W. E. (1969) Optische Bestimmung der gesteinsbildenden Minerale, Teil 2, 2. Auflage, E. Schweizerbart'sche Verlagsbuchhandlung, Stuttgart. 822 pp.
- WINZER S. R., LUM R. K. L., AND SCHUHMAN S. (1976) Rb, Sr and strontium isotopic composition, K/Ar age and large ion lithophile trace element abundances in rocks and glasses from the Wanapitei Lake impact structure. *Geochim. Cosmochim. Acta* **40**, 51–57.
- WOLF S., WOODROW A. AND GRIEVE R. A. F. (1980) Meteoritic material at four Canadian impact craters. *Geochim. Cosmochim. Acta* **44**, 1015–1022.